Universities of Leeds, Sheffield and York
http://eprints.whiterose.ac.uk/

Published paper

Characterisation of white etching crack damage in wind turbine gearbox bearings

T. Bruce, E. Rounding, H. Long*, R. S. Dwyer-Joyce

Leonardo Centre for Tribology, Department of Mechanical Engineering, The University of Sheffield, United Kingdom

*h.long@sheffield.ac.uk

Tel: +44 (0) 114 222 7759

Fax: +44 (0) 114 222 7890

Abstract

White etching cracks (WECs) have been identified as a main failure mechanism of wind turbine gearbox bearings. This study involves the destructive sectioning of a failed low speed planetary stage WTGB and the damage found at manganese sulphide (MnS) inclusions. Inclusions were sectioned through the bearing circumferential and axial directions in order to compare the damage in different directions. 112 damage initiating inclusions were catalogued and their properties investigated.

White etching areas (WEAs) were found at MnS inclusions of lengths 3-45 microns at depths of up 630 microns from the bearing raceway surface and at a wide range of angles of orientation. 29% of catalogued inclusions were internally cracked and 28% were separated from the surrounding steel matrix. Evidence has been found to support the theory that WECs are initiated subsurface, by MnS inclusions, and that butterfly cracks are not necessarily the same features as inclusion-initiated WEAs. Shorter inclusions were found to initiate longer cracks and connected WEAs, as were inclusions that were closer to parallel to the raceway surface in axially sectioned samples.

Keywords

Rolling contact fatigue, Bearings, Optical microscopy, Electron microscopy, Steel

Abbreviations
WTG: Wind Turbine Gearbox
WTGB: Wind Turbine Gearbox Bearing
WEC: White Etching Crack
WEA: White Etching Area
WSF: White Structure Flaking
MnS: Manganese Sulphide
IrWEA: Irregular White Etching Area

1. Introduction

The wind industry faces tough challenges to reduce the cost of wind energy; particularly its high operating cost. The European Wind Energy Agency has a planned target of 230 GW of installed wind power capacity by 2020, representing 20% of total EU electricity consumption [1]. This expansion is being limited due to the expense of a number of maintenance issues, most critically concerning wind turbine gearboxes (WTGs) which are not reaching their anticipated lifespan of 20 years. It is estimated in the UK that operation and maintenance accounts for 20% of the cost of offshore wind energy [2].

The majority of WTG failures initiate in the wind turbine gearbox bearings (WTGBs) [3], and the exact modes of their failure have been intensively researched and widely investigated by industry. White etching cracks (WEC) have been found to lead to premature failure by white structure flaking (WSF) [4], micropitting or by axial cracking [5]. Previous work has identified material defects, particularly manganese sulphide (MnS) inclusions as WEC initiators [6]. This study will investigate damage initiation at manganese sulphide (MnS) inclusions, by destructively sectioning the inner raceway of a failed planetary stage WTGB. Damaged inclusions were catalogued and their properties recorded. The objective was to investigate the different types of damage caused at the inclusions and to find any links between the properties.

1.1. MnS inclusions in bearing steel

MnS inclusions have been classified into three types since 1938 [7]. Type I inclusions are globular in shape and appear in steels with practically no aluminium content. Type II are dendritic chain formations on grain boundaries and appear with the first traces of aluminium (0.005 wt%). Type III are strings of broken silicates and initially appear alongside Type II at levels of 0.01% - 0.03 wt% aluminium. At levels greater than 0.04 wt%, Type III is the only MnS inclusion to appear [7].

Typical bearing steel, such as 100cr6 or 100CrMo7, has negligible aluminium content [8], so it is therefore globular Type I MnS inclusions that are of interest. MnS inclusions in hot-rolled steels are randomly distributed and of irregular shape and are elongated and flattened in the direction of plastic forming [9] during the manufacturing process. Therefore their orientation may vary from bearing to bearing due to differences in the manufacturing process. Three dimensionally, MnS inclusions can be described as long, thin, globular shaped [6].

1.2. White etching cracks

Currently, WTGB failure via WECs is not fully understood therefore bearing life prediction models have yet to be developed to include this failure mode [4, 5, 10, 11] in the selection of bearings. "White etching" refers to the colour of the altered steel microstructure, after having been etched in nital/ethanol [6]. WECs may form irregular crack networks, named irregular white etching areas

(IrWEAs) and follow pre-austenite grain boundaries [5]. These crack networks form up to the depth of maximum shear stress, occurring over large subsurface areas and eventually leading to failure by macropitting. IrWEAs have been observed to propagate radially from straight-growing cracks, which are parallel to the surface in the axial direction. Through-hardened bearings are prone to fail via the axial cracking mode, whereas carburised bearings with less than 20% retained austenite fail by macropitting. Sub-surface cracks occur at various depths and inclinations within the white etching area (WEA) [5]. If this WEA weakens the near-surface of the raceway sufficiently, WSF occurs, leading to failure by spalling. White etching cracking leading to WSF is a mode of damage that can lead to bearing failure within 1-20% of the L_{10} design life [12] predicted by current bearing design standards [13].

WECs have been observed to form from "butterfly cracks", named such due to their two-dimensional appearance. In this case, cracks initiate and propagate between 30-50° and 130-150° from the over-rolling direction, which may be due to the position of maximum Hertzian unidirectional shear stress [4]. These cracks are known as "butterfly wings". During torque reversals caused by tranient loading events, symmetric cracks may form at the same angles, in the direction opposite to overrolling [4].

1.3.   MnS inclusions as crack initiation sites

All inclusions may act as crack initiation sites under high enough contact stress [14], however in the case of white structure flaking in WTGBs, MnS inclusions have been found to be the most likely to interact with white etching crack (WEC) damage [6]. Shorter inclusions have been found to be more likely to initiate damage than longer inclusions, with the ideal length for crack propagation found to be smaller than 20 microns (based on a sample size of 76 WEC-interacting inclusions) [6]. During quenching, the different thermal contraction rates of the bulk material and MnS inclusions may lead to the detachment of the inclusion from the surrounding bulk material, thereby creating a free surface at the subsurface inclusion [14]. The weak interfacial energy bonding MnS inclusions to the matrix may contribute to the creation of this free surface [6]. These free surfaces are potential sites for inclusion separation from the bulk material and for rolling contact fatigue initiated cracking [14]. Cracking has been found to be sensitive to direction within the raceway; with vertical WEC branches appearing to propagate when viewed in circumferential cross-sections and branched that are parallel to the surface in axial cross-sections [6].

Although free surfaces may be potential crack initiation sites, it is not necessary for a MnS inclusion to initiate a crack due to the poor bond with the bulk material. A thin, flattened MnS inclusion may itself act as a virtual crack [15] that may propagate into an actual crack. In rail steel, MnS inclusions can become significant crack initiators [16]. It was found that near to the rail surface, all MnS inclusions were deformed first in the strain direction, moved to the shear angle caused by over-rolling,

and then flattened as they reached the wear surface. Wear tests on four rail steel types confirmed that almost all deformed MnS inclusions near to the wear surface were associated with cracks [15].

MnS inclusions may become elongated under load because they deform more than the surrounding matrix [17][18]. Cracks can be initiated along the highly strain flattened MnS inclusions [17], due to: micro-crack initiation at localised deformation bands in the vicinity of the inclusions; high stress concentration in the middle of the elongated inclusions leading to interfacial debonding and void formation, which are potential crack initiation sites; break up the inclusions causing cracks to form within the inclusion [18], which may go on to propagate into the bulk material [6].

A three-stage process for MnS initiated WEC formation has been proposed [19] and is illustrated in Figure 1, by using the evidence found in this study. Firstly, the inclusion fractures along the length of its major axis; Figure 1(a). Separation of the inclusion from the bulk material may or may not occur. Secondly the crack propagates into the bulk material surrounding the inclusion; Figure 1 (b-c). Finally, white etching areas (WEAs) develop along the cracks; Figure 1 (d). This process is similar to that proposed in [19], but with more extensive cracking in images Figure 1 (c) and (d).
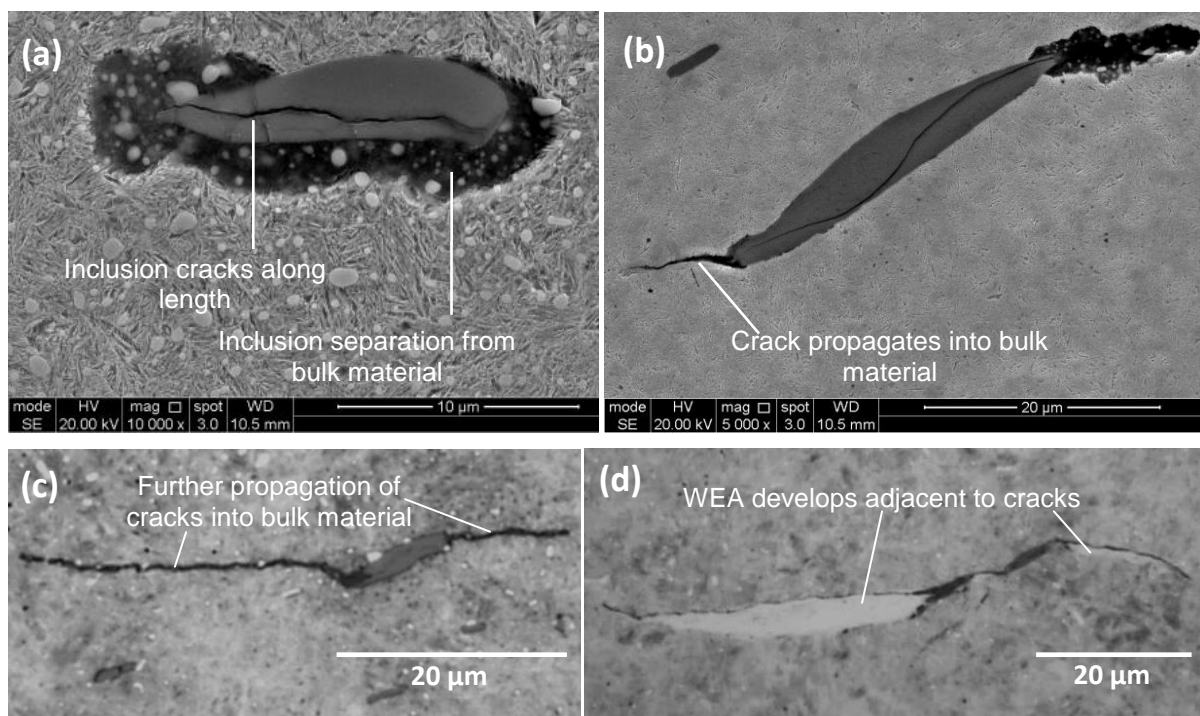

Figure 1: WEA development at MnS inclusions

For a "butterfly" to exist at a MnS inclusion, it was found that the inclusion was always cracked in the direction of the major axis [6] and that the inclusions themselves were initiators of cracks/butterflies that propagated to form WECs. Crack initiation around MnS inclusions and short crack growth can be explained by mode 1 loading (normal to crack growth direction). Further growth of the cracks governed by mode 2/3 shear loading (in-plane shear/off-plane shear) [6].

While it is clear from the results presented in this study that MnS inclusions are WEC initiators, it has been found that it is not necessarily the case that they must be cracked along their major axis in order to do so. WEAs may also form at cracks or free surfaces caused by other previously discussed factors. This is investigated in detail in section 4.

2. Destructive investigation

A failed bearing from the low speed planetary stage of an onshore wind turbine that was operated in the EU was destructively investigated in order to examine subsurface material damage. The wind turbine gearbox had been operating without major incident for five years. A routine oil analysis was carried out 10 days prior to failure, the subsequent report concluding that wear levels were satisfactory and the routine sampling interval should be maintained. The turbine was taken out of service 10 days later when the SCADA control system received the low gear oil pressure alarm. After inspection, it was found that the bearing presented in this study had catastrophically failed. The operating conditions for this bearing are summarised in Table 1.

Motion	Nominally rolling contact. Inner ring stationary with rotational motion of outer ring and cylindrical rollers. Rotational speed of outer ring: 38 rpm. Sliding of rolling elements in unloaded zone.
Loading	Repeated loading of same inner raceway arc. Torque reversals and impact loads known to occur. Misalignment possible. Bearing radial loads in the range of 160-220 kN during normal operation [20].

Table 1: Operating conditions of sectioned bearing

2.1. Observation of surface damage

Wear was evident for approximately 55% of the inner raceway circumference, but within this region the coverage and type of damage changed. Outside this region there was little to no evidence of wear. The variation in damage has been described by three distinct phases as illustrated in Figure 2.

- **Phase 1**: Damage covered most of the raceway width for approximately 20% of the circumference. There was severe macropitting with evidence of material removal from the surface.

- **Phase 2**: There was a transition to decreasing area of damage coverage. Damage was mainly evident on one side of the raceway towards the non-flanged side of the ring. The wear damage was intermittent but well defined at a width of around 20 mm for approximately 35% of the bearing circumference. Within the main 20 mm band of damage there was severe macropitting. There were also smaller wear scars outside of this band around the centre of the raceway.

- **Phase 3**: Non-damaged phase. Over the remaining 45% of the raceway circumference there was very little evidence of damage detectable by eye.
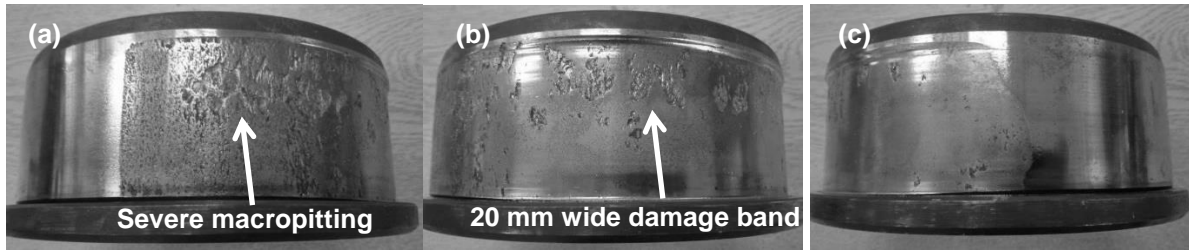
Figure 2: Photographs of raceway damage (a) Phase 1 (b) Phase 2 (c) Phase 3

From the initial observation of the bearing, it seems clear that the failure occurred at some point in the inner raceway, as the outer raceway was relatively undamaged. The inner raceway was therefore selected for investigation. A total of 40 specimens from the three phases were sectioned, compression mounted in a thermoset resin, ground, polished and etched in 0.5% nital in ethanol solution before observation took place.

2.2. Observation of microstructure

From analysing several SEM images such as Figure 3 it has been observed that the predominant fibrous regions are martensite, separated by the darker non-fibrous regions of retained austenite and interspersed with spheroidal carbides. The steel is produced by rapid quenching from above the eutectoid temperature, before tempering at 160 °C. This creates a microstructure containing martensite, about 6 % volume of retained austenite and 3 - 4 % of cementite particles [14]. There were many MnS inclusions throughout the microstructure and their chemical composition was confirmed using Energy Dispersive X-ray Analysis (EDAX) as shown in Figure 4.
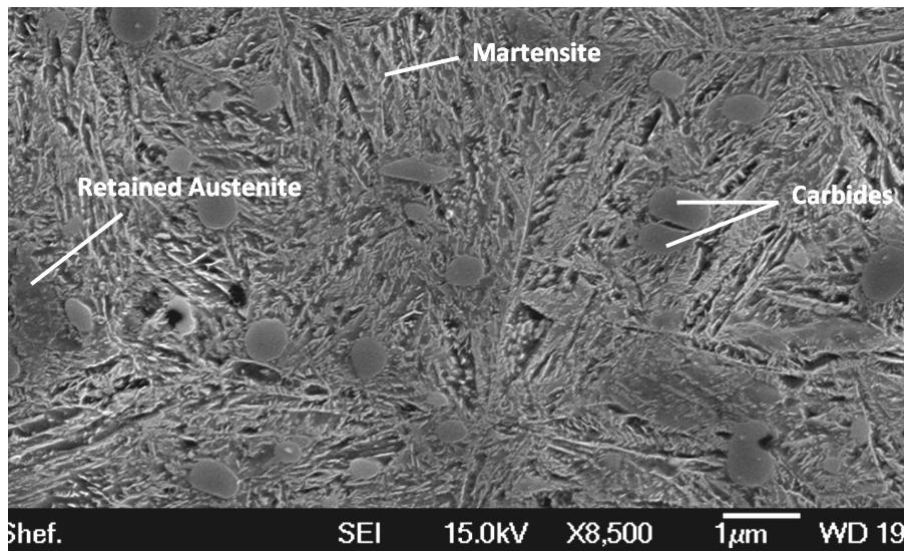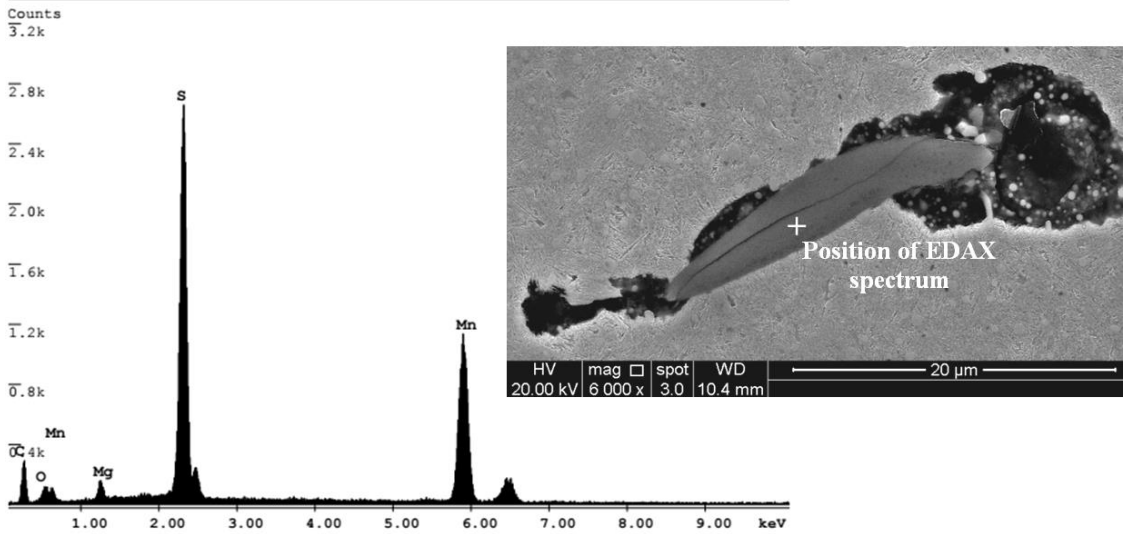

Figure 3: Bearing steel microstucture

Figure 4: EDAX spectrum showing chemical composition of MnS inclusion

3. Key features of found damage

As previously mentioned, the rolling process used during manufacture of the bearing raceways determines the orientation of the MnS inclusions in the steel matrix. In this bearing, inclusions were orientated with their major axis close to parallel with the bearing surface when viewed in an axial cross section as shown in Figure 5a. They were also elongated to a lesser extent when observed in circumferential sections and were generally angled at approximately 30 degrees from the surface tangent as shown in Figure 5b. MnS inclusions were consistently orientated in this manner, regardless of their location in the bearing raceway. As a result, it was necessary to prepare specimens sectioned both axially and circumferentially, in order to determine whether cracks form preferentially in either direction. A summary of the specimens investigated and the damage found at each location is provided in Table 2. 112 damage initiating inclusions were found during sectioning and their properties catalogued will be described in section 4.
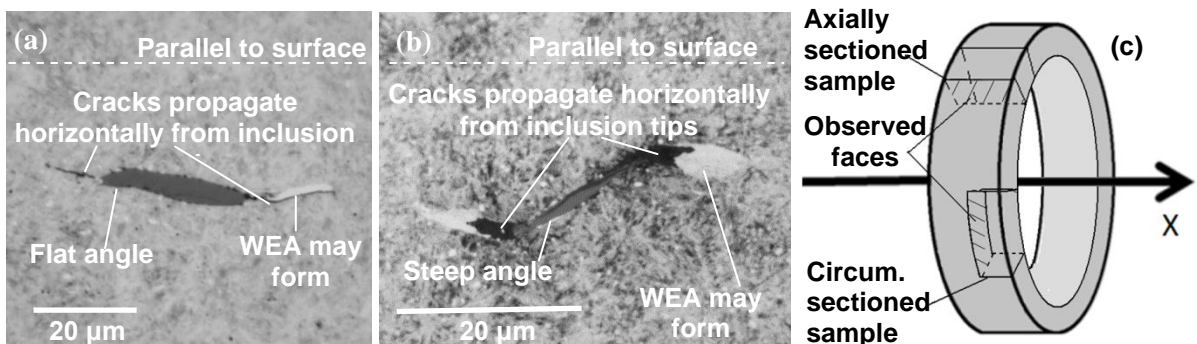

Figure 5: Inclusion orientation in inner raceway a) Typically MnS inclusion viewed axially b) Typical MnS inclusion viewed circumferentially c) Specimen orientation (not to scale)

Section details	Sample Nos.	Observations/Features
Section 1a - Circumferential section. Phase 1 damaged region.	1-6	WEA interacting inclusions Crack initiating inclusions
Section 1b - Axial section. Phase 1 damaged region.	6-12	Separation of matrix from inclusions Butterfly cracks in near surface zone.
Section 2a - Circumferential section. Phase 1/Phase 2 boundary.	13-18	WEA interacting inclusions Crack initiating inclusions Separation of matrix from inclusions
Section 2b - Circumferential section. Phase 1/Phase 2 boundary.	19-24	Butterfly cracks in near surface zone. Significant subsurface crack parallel to the raceway. Substantial WEC propagated vertically down from the surface Surface initiated RCF cracks
Section 3a - Circumferential section. Phase 2 damaged region.	25-30	WEA interacting inclusions Crack initiating inclusions Separation of matrix from inclusions Small butterfly initiated WEC
Section 3b - Axial section. Phase 2 damaged region.	31-36	Large butterfly crack with WEC propagating to surface Surface initiated RCF cracks Plastically deformed region
Section 4a - Circumferential section. Phase 3 non-damaged region	37-40	No evidence of damage

Table 2: Summary of sectioned specimens and damage found

3.1. Distinction of "butterfly" and WEC initiating inclusions

It has become apparent that there has been some confusion over the definition of the term "butterfly" in the literature. The term was originally introduced in order to explain features that appeared to resemble a butterfly, with four "wings", symmetrically propagating from a central point as shown in detail in Figure 6, which gives an example of a series of linked butterflies and connected WECs that propagate to the raceway surface. Highly magnified SEM images of the largest butterfly are presented showing the severe elongation of carbides in the vicinity of the WEA. It is clear that there is no obvious inclusion initiating any of the butterfly features in Figure 6. The butterflies presented in this image clearly have 4 "wings".

Of the 112 catalogued inclusions, 89 inclusions were connected to WEAs. All 89 inclusions had either one or two WEAs that tended to propagate at much shallower angles than traditional "butterfly wings". Most WEA initiating cracks propagated close to horizontally from the inclusion, with the steepest angle not exceeding 30 degrees. It is suggested that WEAs linked to inclusions are not "butterfly wings". Examples of these inclusion-initiated WEAs are shown in Figure 7. The features are thought to be distinct from the butterfly features and should be treated as such, so they will not be referred to as "butterflies" in this study, but as WEA-interacting MnS inclusions.
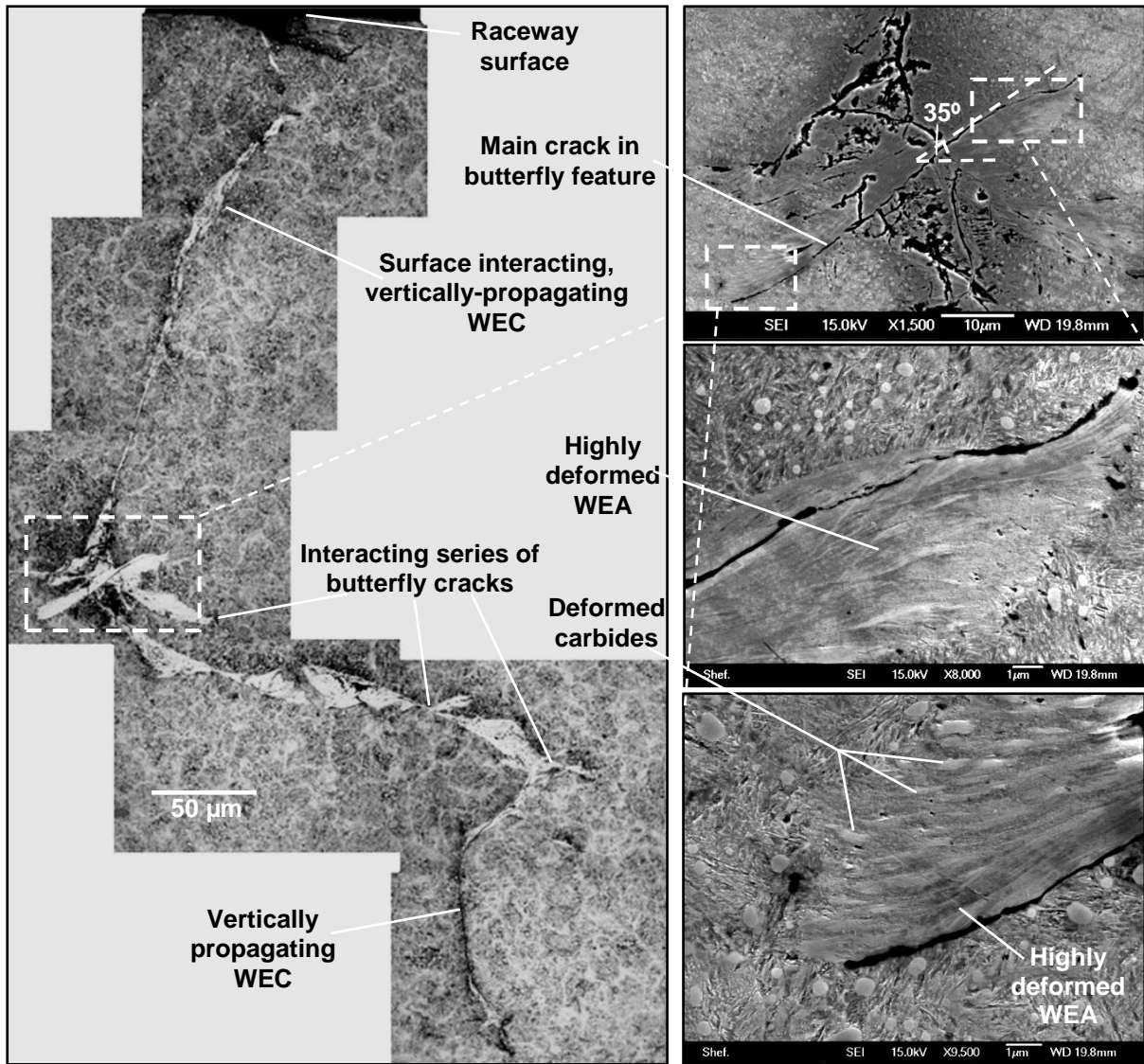
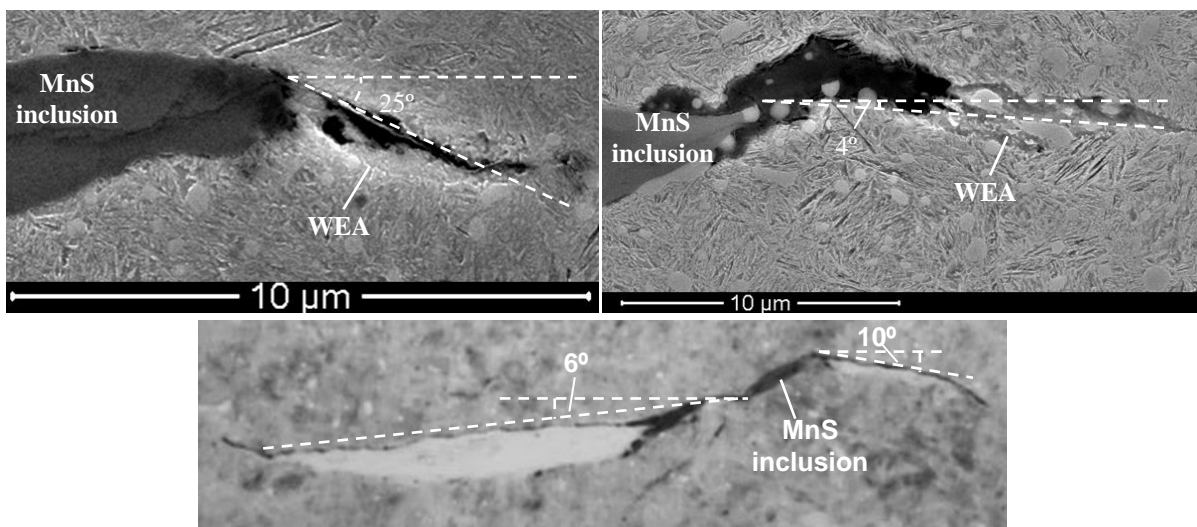**Figure 6: Series of butterflies and connected WECs**

Figure 7: Examples of WEA-interacting MnS inclusions

3.2. Subsurface inclusion-initiated WEC formation

There is debate regarding the location of WEC initiation; broadly there are two arguments:

1. WECs initiate subsurface and propagate up to the surface, leading to failure, either by WSF or axial cracking [4, 21, 22, 23, 14, 24, 6, 12, 25]

2. WECs initiate on the surface and propagate downwards[19], meaning that they are a result of surface failure rather than its cause.

Point 1 and 2 are not necessarily mutually exclusive, however, evidence found in this study certainly suggests that point 1 is correct and that WECs may initiate subsurface, most commonly at MnS inclusions.

Figure 8 presents evidence that such damage is initiated at MnS inclusions. Figure 8a shows three nearby inclusions, which have each independently initiated cracking. They are not part of an extended crack network and no other cracks are visible on this plane, therefore crack initiation must have begun at the inclusions themselves. Figure 8b shows a typical WEA, initiated at an inclusion, around 150 microns below the raceway surface. Again the feature does not appear to be linked to any extended crack network. Since all 112 damage initiating inclusions did not appear to be part of a larger crack network, the evidence that the damage was initiated at the inclusions is conclusive. Figure 8c shows typical cracks formed at the ends of damaged inclusions. The location of crack initiation at the inclusion tips, and at the highest radius of curvature, coinciding with the location of maximum equivalent stress concentration around the inclusion [26], suggesting that it is high stress levels that have initiated cracking.
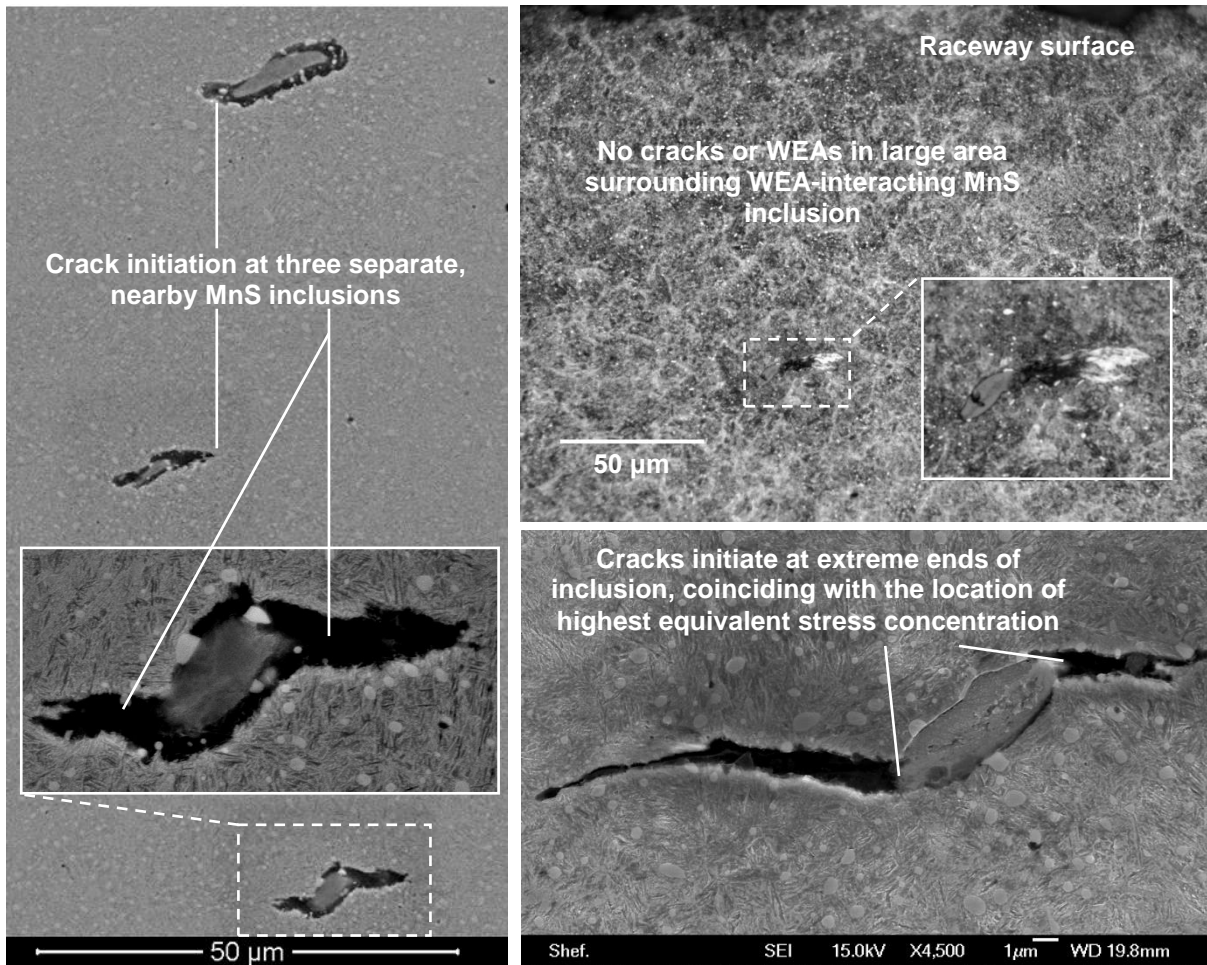
Figure 8: Subsurface inclusion initiated WEAs

It has been reported [27] that MnS inclusions may act as "virtual cracks", which due to their low strength may propagate actual cracks. An example of a MnS inclusion acting as a virtual crack is presented in Figure 9, where the inclusion that is intersected by a large crack network, diverts a crack by a distance of approximately 10 microns. This finding supports the theory that cracks preferentially propagate along MnS inclusions, rather than the surrounding matrix and shows that they are a "weak spot" within the steel microstructure.
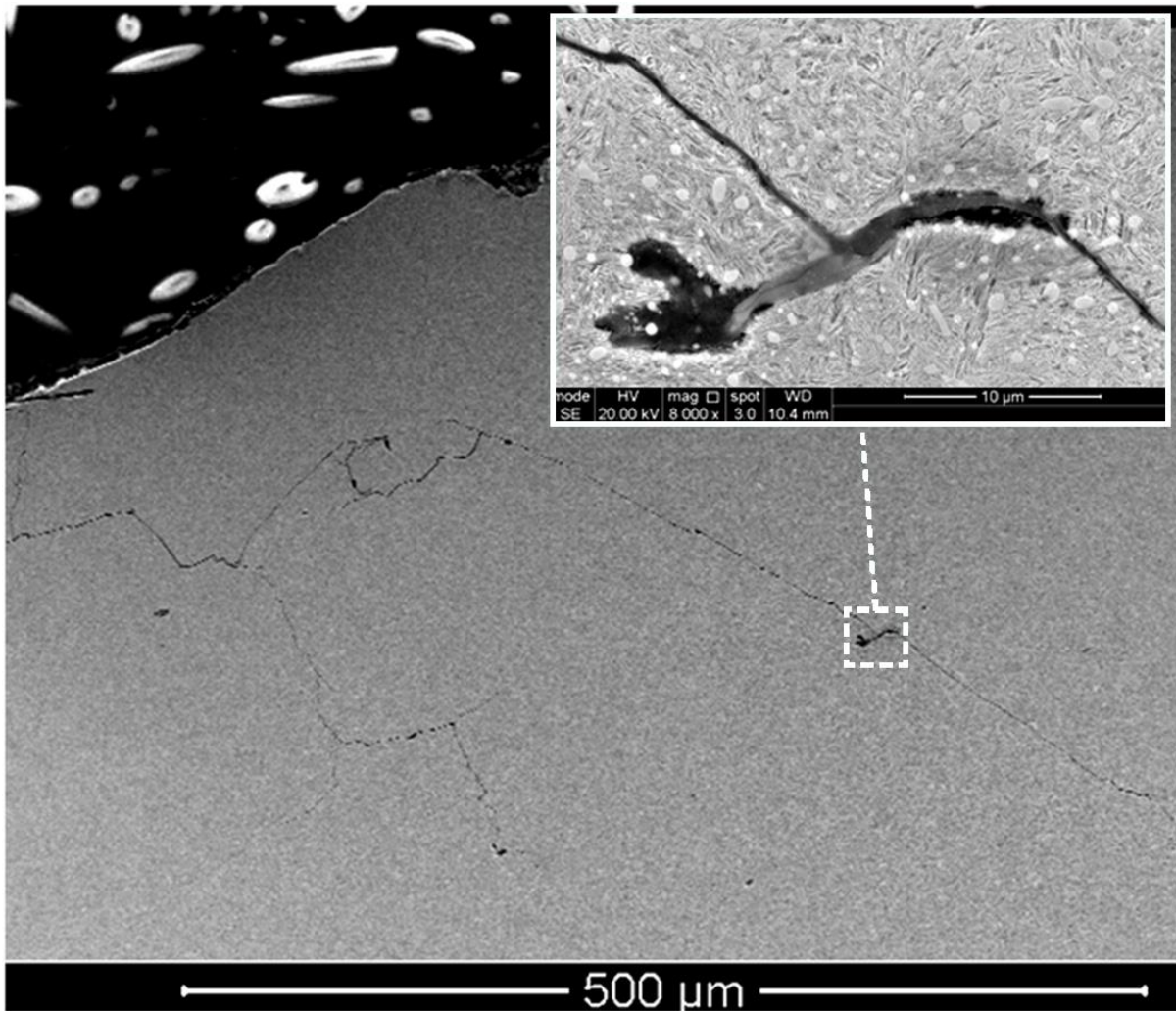
Figure 9: Crack "deflection" by MnS inclusion

3.3. Damage initiation and propagation at MnS inclusions

The observed damage at MnS inclusions found during sectioning is summarised in Figure 10.
Inclusions are initially undamaged and well-bonded to the matrix (stage 0). The first sign of damage
may be internal cracking of the inclusion (stage 1a) and/or separation of the inclusion from the steel
matrix (stage 1b). Cracking may be initiated into the steel matrix (stage 2), possibly from propagation
of the stage 1a internal crack, from stage 1b type separation, or from the inclusion tip that may act as a
stress concentration point. WEAs then form at stage 1b separation (stage 3a) or, at stage 2 type
propagated cracks (stage 3b). Further propagation of cracks and sometimes, of their attached WEAs,
may then take place (stage 4), leading to the propagation of what has been termed white etching
cracks (WECs), far away from the MnS inclusions. The likelihood of each damage type occurring and
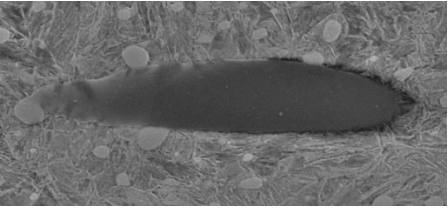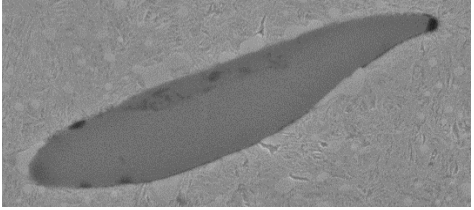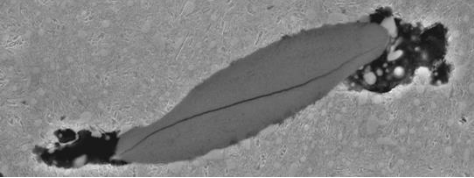the possible relationships between each are investigated in section 4.
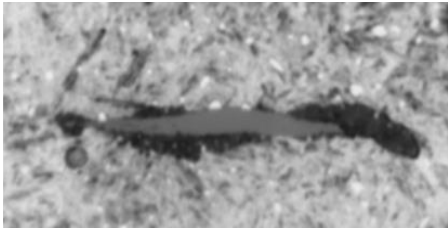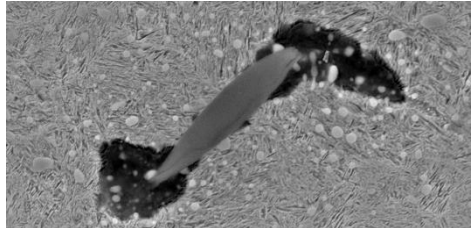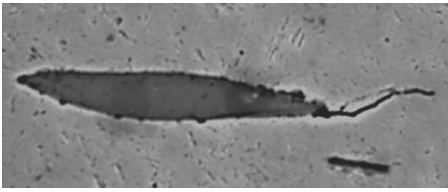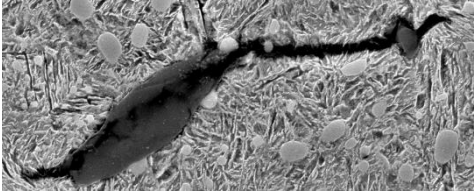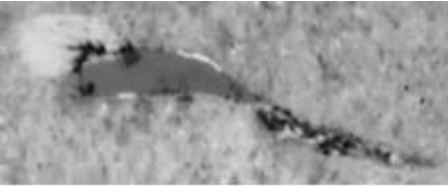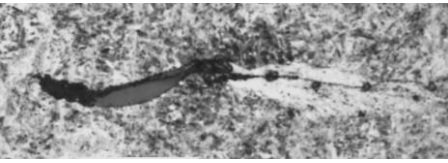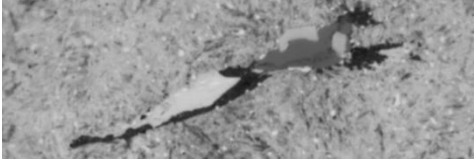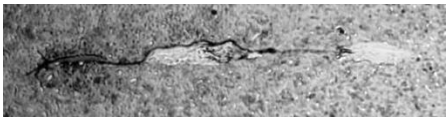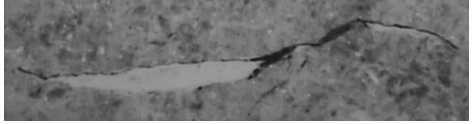
	Axial cross-section shape	**Circumferential cross-section**
Stage 0 Undamaged inclusion		
Stage 1a Inclusion internal cracking		
Stage 1b Separation of inclusion from matrix		
Stage 2 Crack propagation into matrix from inclusion tip		
Stage 3a WEC propagates from separation at inclusion tips		
Stage 3b WEA develops adjacent to cracks		
Stage 4 Further propagation of crack and WEA into bulk material		

Figure 10: Damage initiation and propagation at MnS inclusions

4. Analysis of inclusion properties

112 damage initiating inclusions from circumferentially and axially sectioned samples were identified and catalogued. The following data was recorded, with the aim of finding trends between the different properties. This section discusses links between the damage found, summarised in the previous section.

- Depth from surface
- Angle of inclusion
- Whether the inclusion is internally cracked
- Whether the inclusion is separated from the surrounding steel matrix
- Length of crack initiated from left and/or right end of inclusion
- Length of WEA initiated from left and/or right end of inclusion

4.1. Relationship between damage types at MnS inclusions

Figure 11 shows the relationship between three types or stages of damage at MnS inclusions; internal cracking, separation from the bulk material and WEAs linked to the inclusions. Figure 11a shows that 29% of damaged inclusions were both internally cracked and WEA initiating, while, 50% had initiated WEAs without being internally cracked. This result clearly demonstrates that an inclusion does not necessarily need to be internally cracked in order to initiate a WEA. Similar percentages in Figure 11b show that separation from the bulk material has a similar link to the probability of the inclusion interacting with a WEA, with 28% of separated inclusions being linked to WEAs, and 51% of non-separated being linked. This shows that an inclusion that does not separate from the steel matrix is more likely to initiate a WEA than one that does, perhaps because some stress is relieved by the separation. Figure 11c appears to show no strong prevalence of damage occurring at inclusions that are internally cracked or that are separated from the bulk material, or those that are both cracked and separated.
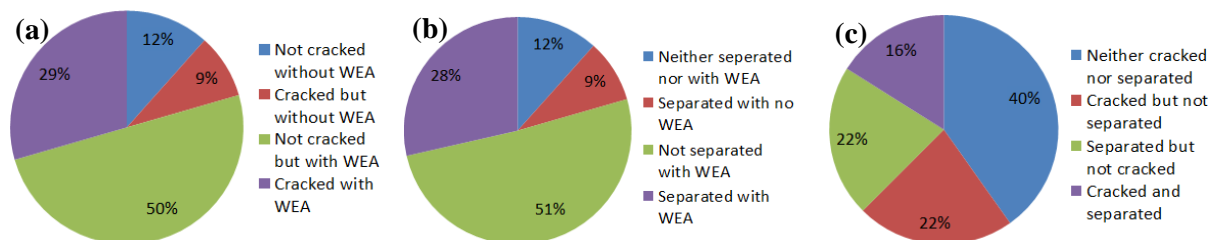

Figure 11: Relationship between damage types (a) internal cracking and WEA formation (b) separation from bulk material and WEA formation (c) internal cracking and separation from bulk material

4.2. Variation of damage with inclusion depth

No trends were found when comparing the angle and the size of inclusions with their depth from the raceway surface, thus it is clear that inclusion distribution is random in the sample bearings and that the effects of over-rolling have little influence on the size and orientation of the inclusions. In addition, WEAs were found on many of the deepest damaged inclusions, to a depth of approximately 600 microns from the raceway surface. It was interesting, however, that no internally cracked or separated inclusions were found deeper than 430 microns. In fact the average depths for inclusions that were internally cracked and for those that had separated from the surrounded bulk material were just 3 microns different (219.5 microns and 216.2 microns respectively). This suggests that inclusion cracking and inclusion separation may be affected by similar initiation mechanisms. These results are outlined in Figure 12.
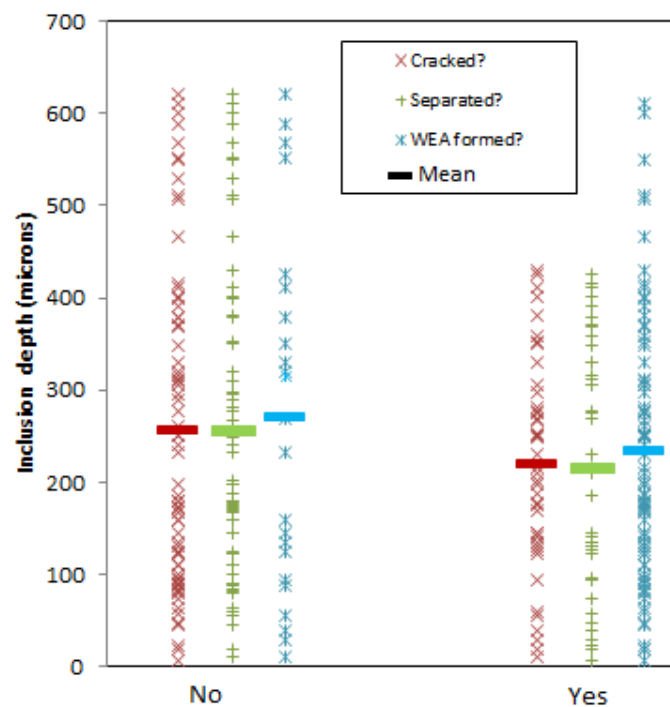

Figure 12: Variation of inclusion damage with depth

4.3. Variation of damage with inclusion orientation angle

No trends were found when properties were compared to inclusion orientation in the circumferential sectioned samples. However Figure 13 shows that the length of cracks propagating in the axial direction was generally greater in "flatter" axially sectioned inclusions. That is to say that it appears that the closer the inclusion's major axis is to being parallel with the bearing raceway surface, the longer the initiated propagated crack is likely to be. This finding suggests that an inclusion is more likely to act as a damage initiator in the axial direction if it is closer to being parallel with the bearing

raceway surface. Figure 13, shows the magnitude of the angle of the inclusion from parallel, that is, the direction of the angle from parallel is not considered.
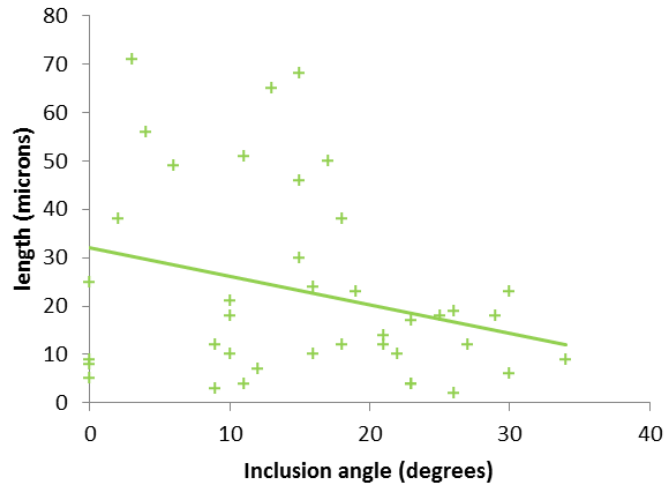

Figure 13: Relationship between inclusion angle magnitude from horizontal and propagated crack length

4.4. Variation of damage with inclusion size

Damage was present on inclusions of all sizes between 3- 45 microns, but trends were found, between the lengths of cracks propagating into the bulk material, connected to inclusions and that of the inclusion interacting WEAs. As shown in Figure 14a, crack length tended to be longer at smaller inclusions for both axially and circumferentially sectioned samples. This is not unexpected as coarser inclusion sizes, in general, have a larger local stress-concentration factor [28]. Similarly, Figure 14b shows that interacting WEAs were generally longer at smaller inclusions for both sample types. The results also show that cracks and WEAs tended to be longer in axially sectioned inclusions than circumferentially, that is, that both forms of damage were more pronounced in the inclusions that were sectioned along their major axis. There was no trend found between inclusion length and the likelihood of internal cracking.
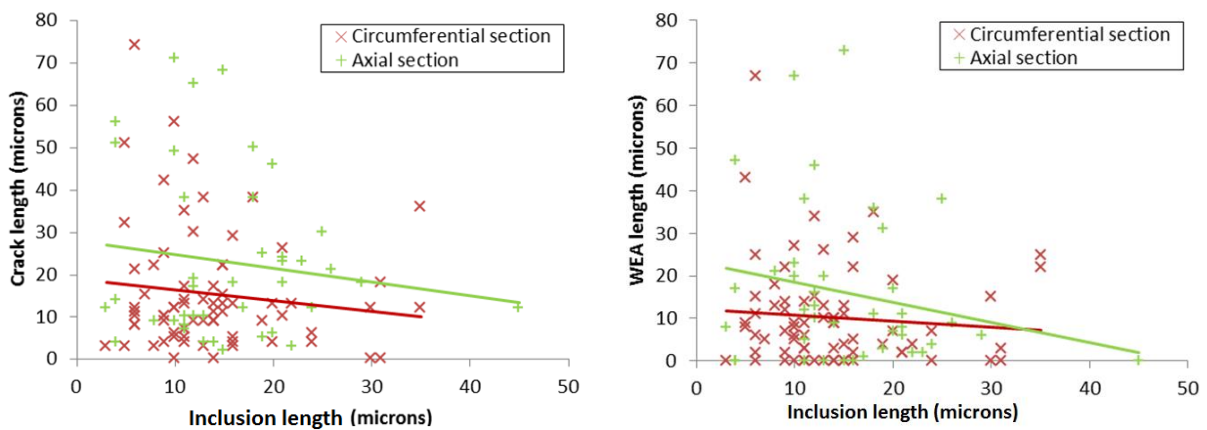

Figure 14: Variation of inclusion damage with inclusion width (a) initiated crack length (b) attached WEA length

Conclusions

By investigating a failed wind turbine gearbox bearing, MnS inclusions were found to have initiated significant levels of damage to the subsurface of an inner raceway of a planetary bearing in a wind turbine gearbox. By observing and cataloging the damage, the following conclusions were drawn up:

1. Four main forms of damage were found at MnS inclusions; internal cracking, crack propagation into the bulk material, separation from the surrounding material and WEA initiation. The 89 MnS inclusions that had connected WEAs found in this study are not the same features as "butterfly cracks", with WECs that propagate at shallower angles than traditional "butterfly wings". The presence of MnS inclusions is certainly one driving factor for subsurface WEC initiation.

2. WEAs often form at MnS inclusions and are usually linked to a crack, propagating from the inclusion, in a direction close to parallel with the raceway surface in the axially sectioned samples. It was found to be more likely for a WEA to form at an inclusion that was not internally cracked (50% of catalogued inclusions), than one that was (29% of catalogued inclusions). It was found to be more likely for a WEA to form at an inclusion that was not separated from the surrounding material (51% of catalogued inclusions), than one that was (28% of catalogued inclusion).

3. Neither internal cracking of inclusions nor separation of inclusions from the surrounding material occurred at inclusions deeper than around 420 microns from the raceway surface, although WEAs were found at inclusions as deep as around 630 microns.

4. Cracks propagating from inclusions tended to be longest when initiated by smaller inclusions of around 0-20 microns in length. When viewed in an axial cross-section, longer cracks were also found from inclusions that were closer to being parallel with the raceway surface, than those that were more steeply angled. In general, cracking was more extensive in the axial direction than circumferentially, although damage propagated significantly in both directions.

Acknowledgements

References

1. European Wind Energy Agency (2010), *The European Wind Initiative 2013* (2013) [Online]. Available: http://www.ewea.org/publications/reports/the-european-wind-initiative-2013/.

2. I. C. Group (2012), *Technology Innovation Need Assessment (TINA), Offshore Wind Power Summary Report.*

3. Musial, W., Butterfield, S. and McNiff, B. (2007) *Improving wind turbine gearbox reliability*, Conference Paper, National Renewable Energy Laboratory, NREL/CP-500-41548.

4. Evans, M. -H. (2005) White structure flaking (WSF) in wind turbine gearbox bearings: effects of 'butterflies' and white etching cracks (WEC), *Materials Science and Technology*, 28(1), 3-22.

5. Errichello, R., Budny, R. and Eckert, R. (2013) Investigations of bearing failures associated with white etching areas (WEAs) in wind turbine gearboxes, *Tribology Transactions*, 56(6), 1069-1076.

6. Evans, M. -H., Ricardson, A., Wang, L., and Wood, R. (2012) Serial sectioning investigation of butterfly and white etching crack (WEC) formation in wind turbine gearbox bearings, *Wear*, 302 (1-2), 1573-1582.

7. Sims, C. and Dahle, F. (1938) Effect of Aluminium on the Properties of Medium Carbon Cast Steel, *AFS Transactions*, 46, 65.

8. British Standards Institution (2005), *PD 970:2005 Wrought steels for mechanical and allied engineering purposes. Requirements for carbon, carbon manganese and alloy hot worked or cold finished steels.*

9. Hihara, L. H, Adler, R. P. and Latanision, R. M. (2013) *Environmental Degradation of Advanced and Traditional Engineering Materials*, Boca Raton, FL: CRC Press, 2013.

10. Luyckx, J. (2011) *WEC failure mode on roller bearings.* Presentation at Wind Turbine Tribology Seminar, Hansen Transmissions.

11. G. L. Doll, *Tribological Challenges in Wind Turbine Technology* (2011) [Online]. Available: http://www.nrel.gov/wind/pdfs/day1_session0_3_uakron_doll.pdf. [Accessed 22 08 2011].

12. Greco, A., Sheng, S., Keller, J., Eridemir, A. (2013) Material wear and fatigue in wind turbine systems, *Wear*, 302(1-2), 1583–1591.

13. International Organization for Standardization (2007), *BS ISO 281: Dynamic load ratings and rating life.*

14. Bhadeshia, H. (2012) Steels for Bearings, Progress in Materials Science, 57, 268–435.

15. Perez-Unzueta, A. J. and Beynon, J. H. (1993) Microstructure and wear resistance of pearlitic rail steels, *Wear*, 162-164 Part A, 173-182.

16. Dhua, S. K., Amitava R., Sen, S. K., Prasad, M. S., Mishra, K. B. and Jha, S. (2000) Influence of nonmetallic inclusion characteristics on the mechanical properties of rail steel, *Journal of Materials Engineering and Performance*, 9(6), 700-709.

17. Liu, C., Bassim, M. and Lawrence, S. (1993) Evaluation of fatigue-crack initiation at inclusions in fully pearlitic steels, *Materials Science and Engineering*, 167(1-2), 108-113.

18. Chard, A. (2011) *Deformation of inclusions in rail steel due to rolling contact, University of Birmingham*, Doctoral Thesis.

19. Gegner, J. (2011) *Tribological Aspects of Rolling Bearing Failures*, InTech, 2011.

20. Guo, Y., Keller, J. and LaCava, W. (2012) *Combined effects of gravity, bending moment, bearing clearance, and input torque on wind turbine planetary gear load sharing*. Conference Paper, National Renewable Energy Laboratory, NREL/CP-5000-55968.

21. Gegner, J. and Nierlich, W. (2011) *The Bearing Axial Cracks Root Cause Hypothesis of Frictional Surface Crack Initiation and Corrosion Fatigue Driven Crack Growth*. [Online]. Available: http://www.nrel.gov/wind/pdfs/day2_sessioniv_2_skf_gegner.pdf.

22. Uyama, H. (2011) *The Mechanism of White Structure Flaking in Rolling*. [Online]. Available: http://www.nrel.gov/wind/pdfs/day2_sessioniv_1_nsk_uyama.pdf.

23. Vegter, R. H., Slycke, J. T. (2009) The Role of Hydrogen on Rolling Contact Fatigue Response of Rolling Element Bearings, *Journal of ASTM International*

24. Grabulov, A., Ziese, U. and Zandbergen, H. W. (2007) TEM/SEM investigation of microstructural changes within the white etching area under rolling contact fatigue and 3-D crack reconstruction by focused ion beam, *Scripta Materialia,* 57(7), 635–638.

25. Kotzalas, M. N. and Doll, G. L. (2010) Tribological advancements for reliable wind turbine performance, *Philosophical Transactions of the Royal Society A*, 368, 4829-4850.

26. Joo, M. S., Suh, D.-W., and Bhadeshia, H. K. D. H. (2013), Mechanical Anisotropy in Steels for Pipelines, *ISIJ International,* 53, 1305-1314.

27. C. Luo (2001) *Modeling the Behavior of Inclusions in Plastic Deformation of Steels*, Royal Institute of Technology, Doctoral Thesis.

28. Canale, L. d. C. F., Totten, G. E. and R. A. Mesquita (2008) *Failure Analysis of Heat Treated Steel Components*, ASM International.